

## **METHOD AND SYSTEM FOR MEASUREMENT AND SELECTION OF MAGNETOSPHERIC AND LITHOSPHERIC SIGNALS OF THE EARTH'S SURFACE**

*Boycho Boytchev*

*Space Research Institute, Bulgarian Academy of Sciences*

### ***Abstract***

*ULF signals are ubiquitous phenomena in the Earth's environment. These signals are of magnetospheric, ionospheric and lithospheric origin. Theoretical considerations concerning ground-based recording of ULF signals are made revealing the usefulness of electric field measurements. An instrument for electric field measurement is described and some preliminary data presented.*

### **1. Introduction**

There are several reasons for measuring electric and magnetic field variations on the ground. First, magnetosphere-ionosphere processes contribute to short-term variations of the Earth's magnetic field that are connected with external sources [1]. Second, we use electro-telluric measurements for geological purposes. Third, the Earth's electric potential variations are often treated as a possible precursor of earthquake events [8]. The frequency range of ULF electric and magnetic fields is less than 5 Hz. ULF electric and magnetic fields in the environment are of both natural and anthropogenic origin. The natural sources are solar activity, the magnetosphere and the ionosphere. The natural ULF fields, although weak, have the ability to penetrate through the atmosphere and the Earth's crust. Industrial fields are usually much stronger but they are confined to localized regions around technical systems (e.g., energy power cables, railway lines, transformer stations, etc.).

## 2. Theoretical Backgrounds

In the ULF range, there are also very long-period pulsations with periods of minutes to hours. Long-period (150-600 s) minute pulsations are observed near the geostationary orbit [3]. Junginger et al. [3] have suggested that these pulsations are solar-wind-driven surface waves that couple the field-line resonances near the geostationary orbit. It is left to future research to clarify whether cavity resonances or compressional oscillations are the modes observed at geostationary orbit. Yumoto [10] has reported Pi2 pulsations of dominant period  $\sim 135$  s at high ( $L = 6.9$ ) and low-latitude ( $L = 1.2$ ) stations. He has concluded that Pi2 pulsations are global phenomena and interpreted them as magnetospheric cavity waves excited in the whole inner region bounded by the plasma sheet. Longer period pulsations (with periods  $T > 600$  s) are usually connected with the oscillations in the ionosphere, produced by magnetospheric (sub)storms, or by influences produced in the lithosphere, or atmosphere (see Sorokin and Fedorovich, 1982). The latter are of electromagnetic nature, i.e., their electric field  $E$  is perpendicular to the propagation direction. These wave phenomena have typical periods of 600 – 6,000 s. They have been defined as gyrotropic waves (GW). These wave disturbances are sometimes transformed into usual magnetohydrodynamic (MHD) modes, otherwise wave disturbances of period  $T > 600$  s are not transformed. The transformation conditions depend on the frequency and the ionospheric state. Inversely, MHD waves of very long period (above 100 seconds) and phase velocity of 10-1,000 km/s cannot penetrate into the ionosphere and the Earth's surface. It is thought that a MHD wave field of a very long period will possess a wavelength that is comparable to the scale size of the magnetosphere. Therefore, geometric effects are to be taken into account. If the latter are considered localized MHD waves of a very great period they could propagate to the ionosphere. In the ionosphere, these modes could partly be transformed into GW as examined by Sorokin and Fedorovich [5]. Thus, on the Earth's surface we could expect ULF disturbances of various origin – from the lithosphere (connected with the active seismic events) or from the magnetosphere.

In this study, we are examining the field properties of long-period disturbances produced on the Earth's surface. We are studying the electric and magnetic field distribution of the ULF wave disturbances in the system lithosphere-atmosphere-ionosphere. We will point out the amplitude differences connected with the sources of the ULF disturbances. We

introduce an electrostatic potential  $\phi$  and a magnetic vector potential  $A$ . According to the physical properties of the different regions, we are going to obtain quantitatively the effects on the electric and magnetic field distribution.

The ULF electro-telluric field is associated with the ULF magnetic field magnitude. The latter could be evaluated according to the relation [4, 6]

$$A = \mu_0 \epsilon_{\text{crust}} \partial \Pi / \partial t + \mu_0 \sigma_{\text{crust}} \Pi, \quad (1)$$

where  $A$  is the magnetic field potential and the Hertz vector  $\Pi_e$  ( $\Pi = -\epsilon_{\text{crust}}^{-1} \Pi_e$ ) is connected with the electric field potential  $\phi$  by the relation  $\phi = \text{div} \Pi_e$ .  $\epsilon_{\text{crust}}$  and  $\sigma_{\text{crust}}$  are the crust dielectric permittivity and conductivity, respectively. In a medium of finite conductivity  $\sigma_{\text{crust}}$  ( $\sigma_{\text{crust}} < \infty$ ) the equation that governs the Hertz vector is

$$\nabla^2 \Pi_e - \mu_0 \epsilon \partial \Pi_e / \partial t - \mu_0 \sigma \partial \Pi_e / \partial t = C \exp(-\sigma_{\text{crust}} t / \epsilon) \quad (2)$$

where  $C$  is a constant. This means that for times  $t > t_0 = \epsilon_{\text{crust}} / \sigma_{\text{crust}}$ , the system will enter steady-state conditions. After  $t_0$ ,  $\Pi_e$  will vary as the magnetic field vector potential  $A$ . Because the vertical current  $\mathbf{j}$  is assumed to be zero, the magnetic vector potential  $A$  has only horizontal components ( $A_x, A_y, 0$ ). (The Hertz's vector  $\Pi_e$  has the same orientation as the magnetic vector potential  $A$ ). In eq. (2), the time derivative is proportional to  $\gamma = -i\omega + k^2 / \mu_0 \sigma_{\text{crust}}$ , where  $\omega$  is the ULF frequency and  $\mathbf{k} = (k, 0)$  is the horizontal wave-vector. According to experimental evidence,  $\omega$  varies from several mHz up to 1 Hz. The fields decay in the Earth with coefficient  $\kappa = (k^2 + i\omega \mu_0 \sigma_{\text{crust}})^{1/2} \cong k$ . Under conditions of long-period pulsations ( $\omega / 2\pi < 0.02$  Hz), the magnetic field potential  $A$  (1) is controlled by the second term. Then, it follows that

$$A \cong \mu_0 \sigma_{\text{crust}} \Pi. \quad (3)$$

Attempting to compare the magnetic field ( $\mathbf{B}$ ) and electric field potential ( $\phi$ ) magnitudes, we obtain the following relations:

$$B_{x,y} = \pm \kappa A_{y,x} \text{ and } \phi = \kappa \Pi_x.$$

$$\text{Hence } |B_{x,y}| \cong \mu_0 \sigma_{\text{crust}} |\phi|. \quad (4)$$

For crust conductivity of  $10^{-2}$  S/m, the magnetic field magnitude will be of the order of  $4\pi \times 10^{-9} \phi$  (in T) (conductivities of  $10^{-2}$  S/m refer to soil conditions). If we use a value of 0.01 V for the observed ULF electric signals, we obtain a magnitude of the order of  $1 \cdot 10^{-10}$  T for the primary ULF magnetic field that penetrates into the soil. Such values correspond to geomagnetic pulsations magnetic field magnitude in the Pc3 range (with period  $T = 10\text{--}45$  seconds). However, under rock conditions, the conductivity is of the order of  $10^{-4}$  S/m. Thus, the primary ULF magnetic field magnitude requires greater electro-telluric field magnitudes. Therefore, under rock conditions, the observation of ULF pulsations is facilitated. In addition to ULF signals of magnetospheric origin, there are ULF electric signals from internal, lithospheric sources [8, 9]. According to eq. (4), the magnetic field magnitude would then be very low and its registration with a magnetometer is likely to be hampered. For this reason, the magnetic field potential  $A$  of the ULF signals of lithospheric origin has to be neglected. This makes preferable the ULF electro-telluric measurements for ULF signals of both the magnetospheric/ionospheric and lithospheric origin. The period of the lithospheric ULF signals varies from twenty minutes to several hours. Thus, ULF signals of magnetospheric origin have higher frequencies than those of lithospheric origin and hence they can be easily separated from each other. This peculiarity is used to design an integrated instrument for measuring ULF signals from internal and external sources.

### 3. Penetration of Signals of Lithospheric Origin

Upon solving the corresponding wave equation assuming homogeneous conductance,  $\sigma_{\text{crust}}$ , an illustration of the electric field amplitude distribution in the lithosphere is obtained (Fig. 1). The conductance  $\sigma_{\text{crust}}$  is assumed to be equal to  $10^{-4}$  S.m. Fig. 1 shows the amplitude decrease (in relative units) versus distance  $r$  for varying frequencies: 0.001 Hz, 0.01 Hz, 0.1 Hz, and 1 Hz. For higher frequencies, the signal decrease is substantially stronger. Fig. 2 demonstrates the dependence of the decrease of a signal of given frequency when the signal penetrates through a medium of varying conductances. Such a dependence has to be observed for the spectral components of aperiodic electric field signals.

The frequency dependence of the ULF signal results in:

*for periodic signals* – different depth of penetration depending on the frequency; thus, signals of higher frequencies could not reach the Earth’s surface and/or would not be detected at the measurement point;

*for aperiodic signals* – change of the spectral content of the signal; the disappearance of the higher frequencies would be observed like a smoothing of the signal envelope. This process depends on the distance between the source and the measurement point.

Following this general outcome, an important conclusion could be drawn. At a measurement point that is displaced at tens, or hundreds of kilometers away from the epicenter of the forthcoming earthquake, or the source of the ULF disturbance that accompanies the earthquake, only aperiodic, or quasi-static signals of large spatial scales and of frequency spectrum strongly limited from above can be detected. Since ULF electric disturbances of smaller scales (less than several km) cannot be periodic [2], at such measurement points, only aperiodic disturbance can be detected.

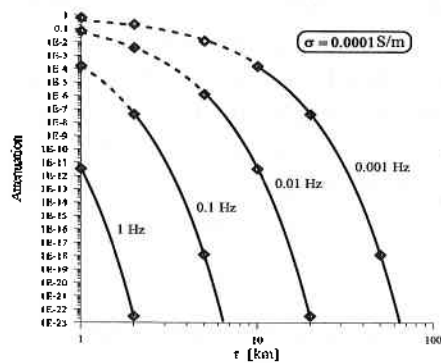


Fig. 1

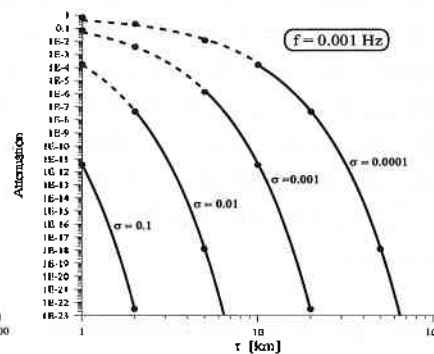


Fig. 2

#### 4. Method of Frequency Selection of ULF Signals

The ULF signals of magnetospheric and lithospheric origin possess similar frequency spectra. The similarity of the frequency spectra suggests a discrimination of the signals using other signal features. A strategy for electric and magnetic field measurements of such ULF signals should rely on the locality of the signals of lithospheric origin and the relative homogeneity of the signals of magnetospheric origin because of the greater scales of the latter. The higher frequency components of the signal generated from the medium will disappear much faster than those of the lower frequency components. It follows that when the distance  $r$  changes, not only the overall amplitude should decrease, but the spectral content of the lithospheric signal should be altered. Irrespectively of the initial

amplitude and the spectral content, the amplitude of the higher components decreases up to  $10^{-3}$  times the amplitude of the lower or zero frequency components for distances of 20–100 km and middle Earth conductance values. The ULF signals of lithospheric origin in the form of Earth electric potential (EEP) variations belongs to a limited frequency band usually below 0.02 Hz and have amplitude range of 0.01-100 mV depending on the lithospheric conductance and the distance between the sensors. As for the study of geomagnetic pulsations of magnetospheric origin, the following frequency interval of measurement is chosen: 0.002–1 Hz [2].

On the basis of the above considerations, a new method of discrimination of the ULF signals is suggested. This method is based on the frequency selection principle [2]. It is suggested that both types of signals be recorded by a common sensor system and common amplification, followed by filtration and treatment in separate frequency ranges. Then:

- At the measurement point, both signals are discriminated in different amplitude ranges. The comparison of their possible maximal amplitudes produces a ratio of  $10^2$  in favour of the lithospheric ones;

- Signals of different genesis are displaced in adjacent frequency regions overlapping in a tight frequency interval. An identification of the signals in the frequency interval where both signals overlap is possible by using additional characteristics depending on their genesis. Here are the different polarization characteristics and the local signature of the lithospheric signal.

### **5. Description of the Equipment and Operational Flow-Chart**

We are presenting an instrument designed for selective measurement of the electric and magnetic components of ULF signals of lithospheric and magnetospheric origin at the Earth's surface. The electric pulsations are measured in DC – 1 Hz frequency range. Due to the large amplitude variations of the signals, the whole DC - 1 Hz frequency range is divided into 2 sub-bands: DC - 0.02 Hz (BW1) and 0.002 - 1 Hz (BW2). This allows for parallel processing of the signals from both sub-bands. Magnetic components are measured in BW2 sub-band only. Both the magnetic and the electric signals are measured in the East-West and the North-South direction. The instrument consists of sensors, analogue module, digital interface block, IBM compatible PC, and a modem. The instrument allows for:

1. Stand-alone operation at remote sites.
2. Multi-point synchronized observations and centralized data acquisition.

**Sensors.** The electrical sensors are corrosion-resistant metal bodies, buried in the ground. Depending on the soil's composition and the level of moisture saturation, the contact sensor-ground resistance varies in the range  $50 \Omega$  -  $50 \text{ k}\Omega$ . The sensors are placed at a distance of several hundreds of meters from each other and from the instrument. The magnetic sensors are separate units with their own power supply.

**Analogue Module.** The analogue module is galvanically decoupled from the digital module and the PC through optocouplers, with a separate power supply. The overall flow-chart is shown in Fig. 3. The analogue module deals with the correct reception, amplification and subsequent discrimination of the signals derived from the electric and the magnetic sensors. The signals are divided into 2 sub-bands and converted into digital pulses of varying frequencies. The input resistance ( $R_{in}$ ) of the electric sensors is greater than  $10^{12} \Omega$ . The filter (F) suppresses parasite signals outside the active DC-1 Hz bandwidth, especially those from industrial power lines 50 Hz/60 Hz and their respective harmonics. The Instrumentation Amplifier (IA) provides the signal difference between each pair of electric sensors for further processing. The Low Pass Filters (LPF), High Pass Filters (HPF) and the Amplifier (A) divide the signals from each pair of electric sensors into two sub-bands. The same procedure is followed for the signals from the magnetic sensors in the BW2 band. Each of the analogue signals is then converted into pulse sequences of varying frequencies, using Voltage-Frequency Converter (VFC) and then fed into the digital module via optocouplers (O).

**Digital module.** The digital module works as a frequency meter. The number of pulses in each pulse sequence, counted within a time frame of 0.1 s, defines the instant frequency of the respective channel. The digital module converts the instant frequencies into 12 bit words and stores them in the PC. The sampling rate of the BW1 range is 1/60 Hz, while that of the BW2 range is 5 Hz. The digital module is designed in such a way as to be directly integrated into the IBM AT PC. The digital module also generates commands controlling the calibration of the analogue module. In Fig. 3, the digital module is marked as INTERFACE

A supporting software package is developed to assure to proper functioning of the instrument. It consists of software, supporting the measurements (MS) and software, supporting the data acquisition (DAS).

MS performs the real-time astronomic synchronization and re-scaling of the measured signals and their storage in the local PC. MS provides a visualization of the measured signals from BW2 bands in the last 90 seconds and the signals from BW1 bands in the last 9 hours. DAS is responsible for acquisition and collection of the data from all measurement sites. DAS supports an operational database. The software package supports the transfer of data from the measurement sites and acquisition center through modems.

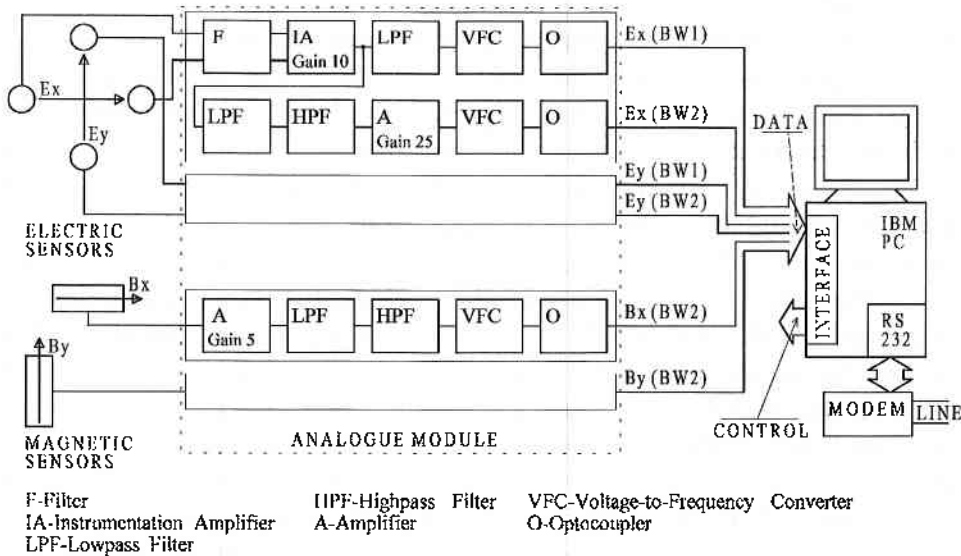


Fig. 3 The instrument's operational flow-chart.

## 6. Summary of the Instrument's Technical Characteristics

1. The input electric signals are differential voltage between two sensors placed in the ground at a distance of 100–500 m. The electric sensors are connected to the instrument by isolated non-shielded wires. The magnetic sensors, placed at a distance of 25 m from the instrument, are connected by shielded cables.

2. Dynamic range and frequency range:

2.1. The dynamic range of the quasi-static electric signals in the frequency band  $DC \div 0.02 \text{ Hz}$  is  $-0.5 \text{ V} \div +0.5 \text{ V}$ .

2.2. The dynamic range of the electric signals in the frequency band  $0.002 \text{ Hz} \div 1 \text{ Hz}$  is  $-0.02 \text{ V} \div +0.02 \text{ V}$ .



2.3. The dynamic range of the magnetic field signals in the frequency band  $0.002 \text{ Hz} \div 1 \text{ Hz}$  is  $-2 \cdot 10^{-6} \text{ T} \div +2 \cdot 10^{-6} \text{ T}$  with resolution:  $\pm 1 \cdot 10^{-9} \text{ T}$ .

### 3. Filtering and electromagnetic compatibility:

The input filter (F) consists of two parts with a buffer repeater between them. The entire damping for disturbances in sin-phase with a power-line frequency of 50 Hz exceeds 100 dB.

## 7. Observational Data

The periodograms, shown in Figs. 4 and 5 for daytime and nighttime conditions respectively, illustrate the evidence of long-period pulsations observed by the measuring system. The spectrum in the figures is obtained during daylight and night hours. The daylight spectrum consists of three periods:  $\sim 300$ , 600 and 900 s. The spectral component with period  $T = 300$  s is the most intense one. Under night conditions, the periods of the spectral components increase to 1,000 s and more.

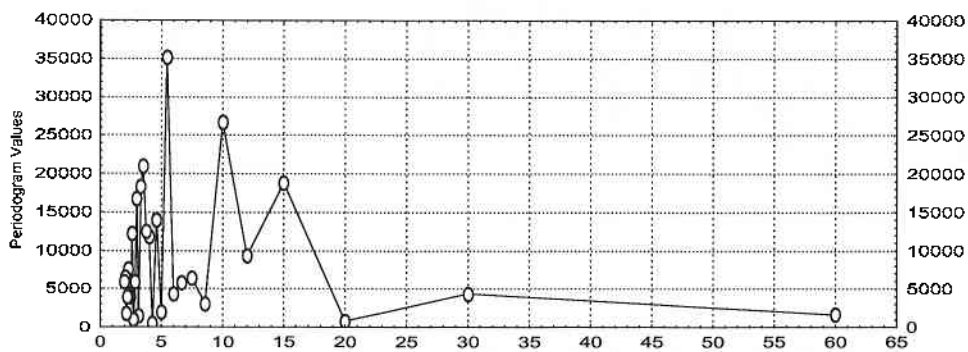


**Fig. 4** Periodogram of day-hour pulsation (Period in minutes). Pulsations of period  $\sim 5$  min and their harmonics at 10 and 15 min are clearly observed.

Our preliminary data set reveals the existence of geo-electric pulsations in the 60–1,800 s range. The period of these pulsations appears to vary from day to day. This means that the processes responsible for their generation have a time scale of several hours or less. Our preliminary conclusion is that their energy source is probably of ionospheric origin.

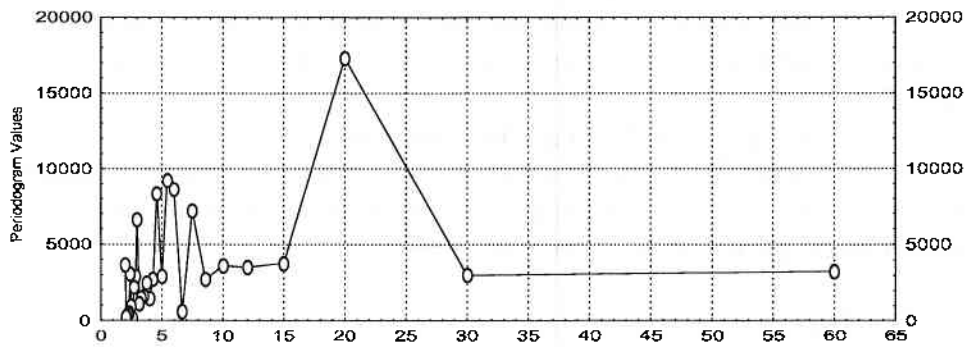


**Fig. 5** Periodogram of night-hour pulsation (Period in minutes). Pulsations of period 20 min are observed.

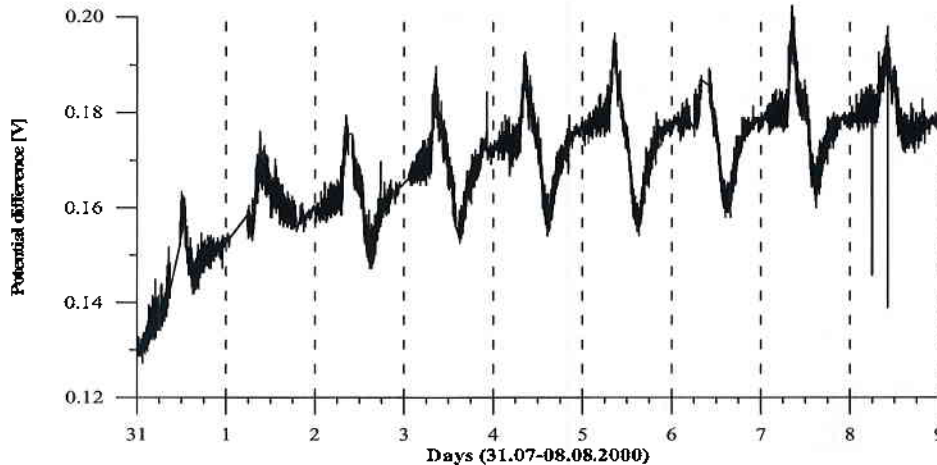


**Fig. 6** Long-term drift of the Earth quasi-static electric potential.

Another feature of our ULF measurements during July 27 – August 08, 2000, is a slow increase (drift) of the magnitude of the Earth's electric potential  $\phi$  (Fig. 6). This drift (measured over the whole interval) does not exceed the diurnal (regular) variations and is less than 20–30 percent of the mean potential. Ralchovski and Komarov [7] have already observed long-term drifts of the Earth's electric potential. A long-term change in  $\phi$  at the same station (Vitosha) has had nearly half-a-month duration before the Vrancea earthquake in March 1986. This could be ascribed to possible changes in the Earth's conductivity during earthquake preparation processes. Our Earth electric potential drift is followed by two earthquakes of magnitude  $M > 5$  which occurred on August 23, 2000, in Vrancea

(Romania) and Izmir (Turkey). Although our data set shows the same feature as in March 1986, the data set is insufficient to connect this drift to lithospheric conductivity changes.

### 8. Conclusion

We have provided theoretical grounds for the advantage of recording the electric field of ULF signals of both ionospheric (magnetospheric) and lithospheric origin.

We have designed an instrument that includes two principal measuring tracks: first, quasi-static geo-electric variations (originating from the magnetosphere and/or lithosphere) superimposed on the diurnal changes in pulsation dynamics; second, ULF geo-electric variations of periods 0.002 Hz to 1 Hz. It provides ULF wave measurements of higher sensitivity.

We have recorded ULF oscillations of period 300–1,200 s from both measurement tracks. Our preliminary conclusion is that these oscillations have unstable periods.

### References

1. Akasofu, S. I., S. Chapman, Solar-terrestrial physics, Oxford Univ. Press, Oxford, UK, 1972.
2. Boytchev, B. V., Methods and means for measurement of low-frequency electromagnetic fields of magnetospheric and lithospheric origin, PhD Thesis, Space Research Institute, Sofia, Bulgaria, 2003. (In Bulgarian)
3. Junginger, II., A statistical study of wave Pointing vectors measured during long-period magnetospheric pulsations at geostationary orbit, *J. Geophys. Res.*, **90**, 8301-8307, 1985.
4. Semenov, A. A. *Theoriya elektromagnitnykh voln*, Moscow University, Moscow, 1968. (In Russian)
5. Sorokin, V. M. Fedorovich, G. V., *Fizika bavnih magnitogidrodinamicheskikh voln v ionosfernoi plazme*, Energoizdat, Moscow, 1982. (In Russian)
6. Stratton, J. A., *Electromagnetic Theory*, Mc Graw-Hill, New York, NY, USA, 1941.
7. Ralchovskii T., L. Komarov, The Vrancea earthquake of 31.08.1986 and Its Possible Electrical Precursors, *Bulg. Geophys. J.*, **13**, 59-64, 1987.
8. Varotsos, P. M. Lazaridou, Latest aspects of earthquake prediction in Greece based on Seismic Electric Signals I, *Tectonophysics*, **188**, 321-347, 1991.
9. Varotsos, P., K. Alexopoulos, M. Lazaridou, Latest aspects of earthquake prediction in Greece based on Seismic Electric Signals II, *Tectonophysics*, **224**, 1-37, 1993
10. Yumoto, K., Magnetospheric cavity resonances waves associated with substorm, *Proc. Japan. Acad.*, **65**, Ser. B, 53-56, 1989.

# МЕТОД И АПАРАТУРА ЗА ИЗМЕРВАНЕ И СЕЛЕКЦИЯ НА МАГНИТОСФЕРНИ И ЛИТОСФЕРНИ СИГНАЛИ НА ЗЕМНАТА ПОВЪРХНОСТ

*Бойчо Бойчев*

## Резюме

В работата е направено изследване на параметрите на литосферните и индуцираните магнитосферни сигнали в земната повърхност. Изследвано е затихването на сигналите при тяхното разпространение. Предложен е метод за едновременното им измерване и селекция. Представени са и детайлно описани измервателна апаратура и система за многоточкови измервания реализиращи този метод. Представени са данни от измерванията, илюстриращи работата на апаратурата на два измервателни полигона.